Radiative Cooling of a Small Metal Cluster: The Case of V_{13}^+

C. Walther,[1,*] G. Dietrich,[1] W. Dostal,[1] K. Hansen,[2] S. Krückeberg,[2] K. Lützenkirchen,[1,†] and L. Schweikhard[2]
[1]*Institut für Kernchemie, Johannes Gutenberg-Universität, D-55099 Mainz, Germany*
[2]*Institut für Physik, Johannes Gutenberg-Universität, D-55099 Mainz, Germany*
(Received 22 March 1999)

Size-selected stored metal cluster ions, V_{13}^+, have been heated by photoexcitation ($\lambda = 730$ to 229 nm) to well-defined excitation energies corresponding to temperatures between 1000 and 2100 K. A millisecond pump-probe photodissociation technique was applied to measure the time-resolved radiative cooling. The observed decay rates are directly related to the radiative energy loss and are explained quantitatively by the competing processes of photoemission and atom evaporation.

PACS numbers: 36.40.Vz, 44.40.+a, 82.80.Ms

Radiative cooling of clusters can be regarded as the microscopic analog of black body radiation. However, in contrast to a macroscopic black body the wavelength of the emitted light exceeds the dimension of its source (the cluster) considerably. Furthermore due to the small heat capacity of clusters, the light emission is suppressed for these particles at high photon energies. Although these effects yield a modification of Planck's law the resulting emission spectra are still smooth as observed in the case of refractory metal clusters (W,Re,Nb) [1,2] and C_{60} [3]. In order to obtain sufficient signal intensity in the metal cluster studies, it was necessary to work with a broad distribution of cluster sizes. In addition, the internal energy of the radiating clusters was not well defined. Only in the case of carbon clusters [4] and C_{60}, where macroscopic amounts are available, radiative cooling of a single cluster size has been investigated [5–8], however in all cases for broad thermal distributions.

In this Letter we present an alternative approach to measure radiative cooling of clusters. It is based on the storage of clusters in a Penning trap and subsequent photoabsorption which allows one to prepare an ensemble of one cluster size at a well-defined temperature. Their radiative cooling is monitored time resolved via its influence on the fragmentation behavior. The data are compared to a Monte Carlo simulation, where atom and photon emission is described by phase space theory [9] and also multiple photon emission is taken into account.

The Mainz Cluster Trap [10] combines an external ion source with a Penning trap–time-of-flight (TOF) mass spectrometer [11]. For the present measurements positively charged clusters are produced by laser vaporization of a vanadium wire and condensation in a helium gas pulse. They are guided towards a Penning trap and stored by a superposition of a homogeneous magnetic field ($B = 5$ T) for radial and an electric quadrupole field for axial confinement (potential well of 1.5 eV). From the ensemble of captured vanadium cluster ions V_{13}^+ is mass selected by radial ejection of all other ions. The V_{13}^+ ions are centered by a combination of buffer gas collisions and quadrupolar excitation [12] and confined within a region of about 1.8 mm diameter in the middle of the trap [13]. In this process the clusters undergo some 300 collisions with argon atoms and equilibrate to a canonical ensemble at room temperature corresponding to $E_0 = 0.53(14)$ eV internal energy. The thermal spread of 0.14 eV is the only uncertainty in internal energy that needs to be considered, even after photoexcitation. 20 ms after laser irradiation the charged reaction products are axially ejected for TOF mass analysis. The duration of the experimental cycle is 1400 ms. Typically, the data of 200 cycles (each with 20 to 50 V_{13}^+ clusters) are added to obtain statistically significant signal intensities. The cycles are alternated with reference cycles (see below), thus providing a quasisimultaneous normalization signal.

To investigate the radiative cooling of the stored clusters we apply a pump-probe technique in the microsecond to second time regime [14]: After the clusters are centered and thermalized as described above they are stored for a delay period of 1 s in order to reduce the buffer gas pressure to below 10^{-8} mbar. Then the light of two pulsed dye lasers ($\lambda = 730$ to 229 nm) is focused axially into the Penning trap. The beam characteristics (profile, position relative to the trap center, pulse energy) are monitored on-line by a charge-coupled device camera. As illustrated in Fig. 1 the cluster is first excited by the

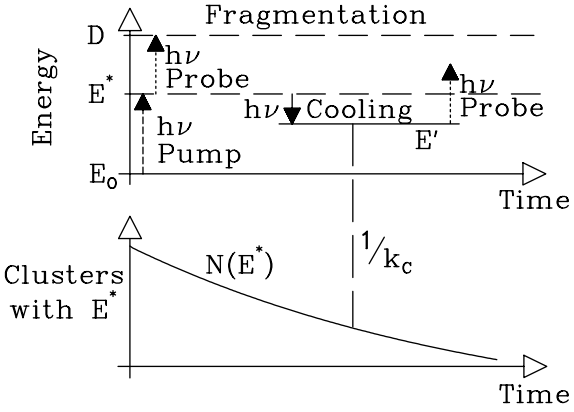

FIG. 1. Top: Energy diagram demonstrating the experimental method (for details, see text). Bottom: Number of clusters with excitation energy E^* as a function of time after photoexcitation with the absorption of $h\nu_{\text{pump}}$.

 0031-9007/99/83(19)/3816(4)$15.00

pump-laser pulse to $E^* = h\nu_{\text{pump}} + E_0$. Absorption of an additional photon of the second laser pulse ($h\nu_{\text{probe}}$) leads to further cluster heating. The following storage period of 20 ms is sufficiently long to allow for the decay $V_{13}^+ \rightarrow V_{12}^+ + V$. The time-resolved fragmentation [15] shows that its half-life increases monotonously with decreasing excitation energy from 35(5) μs at $E^* = 8.5$ eV to 215(70) μs at $E^* = 7.5$ eV. At the same time the fragmentation yield decreases and therefore fragmentation can no longer be observed below $E^*_{\text{thresh}} = 7.5$ eV because it is strongly suppressed in favor of radiative cooling.

If the probe pulse is delayed with respect to the pump pulse by a period Δt the clusters may emit one or more near infrared or visible photons during that period and E^* is reduced to E'. Thus, the fragmentation rate and consequently the observed number of V_{12}^+ fragments is reduced (Fig. 1, bottom). Hence, by monitoring the fragment yield as a function of Δt the radiative cooling after the first photon absorption is measured. The decrease of the fragment yield with increasing delay time is direct and model independent evidence that these clusters cool through radiation.

Furthermore, in order to map the radiative cooling's dependence on the temperature, the pump-photon energy is varied, with the sum of $h\nu_{\text{pump}}$ and $h\nu_{\text{probe}}$ kept constant at 7.71 eV. Thus, when no radiative cooling occurs, the internal energy is $E^*_{\text{max}} = E_0 + h\nu_{\text{pump}} + h\nu_{\text{probe}} = 8.24(14)$ eV.

Typical examples of the observed fragment yields as a function of Δt are given in Fig. 2. The left part shows data taken at $h\nu_{\text{pump}} = 5.01$ eV. Measurement cycles are alternated with reference cycles at $\Delta t = 0$, i.e., simultaneous laser pulses, in order to account for fluctuations of laser fluence or cluster production rate; the fragment yield is normalized with respect to the reference value. The Δt dependence of the fragment yield is well represented by an exponential

$$Y = a + (1 - a)\exp(-k_C \Delta t)\,. \tag{1}$$

The offset a is due to clusters fragmented by multiple absorption of pump photons. The cooling rate of this particular example is $k_C = 2440(400)\ \text{s}^{-1}$. The inverse, k_C^{-1}, is the average time the cluster needs to cool by $\simeq 0.7$ eV ($= E^*_{\text{max}} - E^*_{\text{thresh}}$). The data of Fig. 2 (right), taken at $h\nu_{\text{pump}} = 1.74$ eV, reveal a decay rate of $k_C = 48(5)\ \text{s}^{-1}$. For these energies (below half the fragmentation threshold) two photon absorption leads to a biexponential decay curve rather than creating an offset. Hence the photon fluence was kept very low (two photon absorption probability $<1\%$). The pronounced drop of k_C with decreasing pump-photon energy and thus E^* is in line with the expectation based on the macroscopic black body radiation (where the emitted power is proportional to T^4).

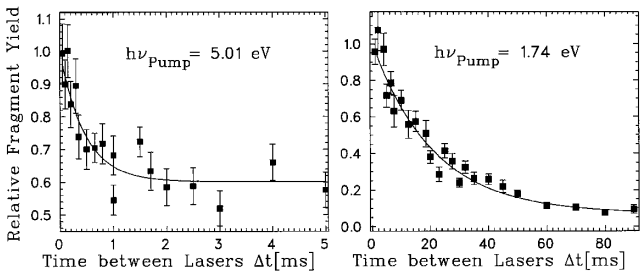

FIG. 2. Fragment yield as a function of the delay period between pump and probe laser pulses for $h\nu_{\text{pump}} = 5.01$ (left) and $h\nu_{\text{pump}} = 1.74$ eV (right).

Figure 3 shows k_C as a function of the clusters' internal energy $E^* = h\nu_{\text{pump}} + E_0$ with $h\nu_{\text{pump}}$ between 1.7 and 5.4 eV. The cooling rates increase almost exponentially from $k_C = 30\ \text{s}^{-1}$ to above $6000\ \text{s}^{-1}$, respectively.

In order to interpret these results quantitatively, emission rates of photons and atoms are calculated as a function of the cluster excitation energy on the basis of detailed balance considerations. For atom evaporation a rate closely analogous to the Weisskopf rates for neutron emission from hot nuclei is found [16–18],

$$k = g\,\frac{m}{\pi^2\hbar^3}\,\sigma T_f^2\,\frac{\rho_{12}(E - D_{13})}{\rho_{13}(E)}\,, \tag{2}$$

where g is the fragment channel degeneracy, m the reduced mass of the fragment/daughter system, σ the atom capture cross section for the inverse process (assumed equal to the geometrical cross section), T_f the temperature after evaporation [defined via Eq. (9)], $\rho_N(E)$ the level density of a cluster of size n at energy E, and D_{13} the dissociation energy of V_{13}^+. The spectral photoemission rate is found by similar considerations [19] to be

$$k_{\text{ph}}(E, h\nu)d\nu = \frac{8\pi\nu^2}{c^2}\,\sigma(E - h\nu, h\nu) \times \frac{\rho_{13}(E - h\nu)}{\rho_{13}(E)}\,d\nu\,. \tag{3}$$

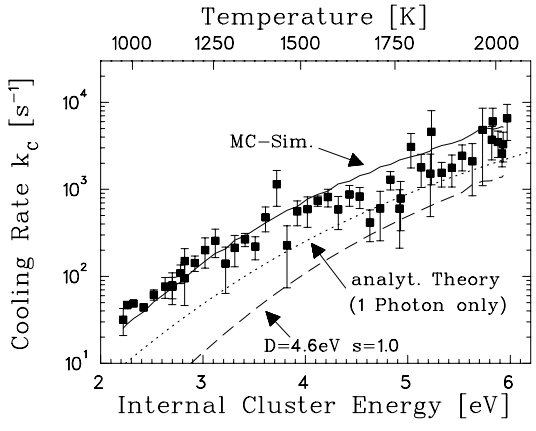

FIG. 3. Radiative cooling rates as a function of cluster energy: Measured values (filled squares) and calculations by Eq. (4) (dotted line) and Monte Carlo simulations (solid and dashed lines).

Integration over the frequency ν gives the total photon emission rate at that particular cluster energy E,

$$k_{\mathrm{ph}}(E) = \int_0^\infty k_{\mathrm{ph}}(E, h\nu)\, d\nu\,. \tag{4}$$

$\sigma(E - h\nu, h\nu)$ is the cross section for absorption of a $h\nu$-energy photon at internal energy $E - h\nu$. Recently, the absorption cross section of V_{13}^+ was measured for $h\nu > 1.5$ eV [20]. The cross sections were found to be independent of internal energy if the cluster is heated above room temperature, i.e., $\sigma(E - h\nu, h\nu) = \sigma(h\nu)$. They are in good agreement with Mie theory [21],

$$\sigma_{\mathrm{Mie}}(\lambda) = \frac{18\pi V}{\lambda} \frac{\epsilon_2}{(\epsilon_1 + 2)^2 + \epsilon_2^2}\,, \tag{5}$$

where V is the particle volume derived from the bulk density of vanadium [22], and $\epsilon_1(\lambda)$ and $\epsilon_2(\lambda)$ are the real and imaginary components of the bulk dielectric function, respectively [23]. The Mie values are therefore also tentatively applied for photon energies below 1.5 eV where to our knowledge no absorption cross sections have been measured. Along with the level densities derived below, this allows one to calculate the spectrum [Eq. (3)] of photons emitted by a cluster of energy E. For instance, at $E = 2$ eV the average photon energy amounts to $\overline{h\nu} = 0.39$ and increases to $\overline{h\nu} = 1.16$ eV at $E = 8$ eV.

The level densities in Eqs. (2)–(4) are found by extrapolation from bulk values as in [17,18]: The heat capacity of vanadium between 298 and 2190 K is [24]

$$C_P(T) = n_{\mathrm{eff}}(b + 2cT)\,, \tag{6}$$

where $b = 2.1038$, $c = 6.353/\mathrm{eV}$, T is expressed in eV ($k_B = 1$), and $n_{\mathrm{eff}} = (3n - 6)/3 = 11$ for $n = 13$ and $n_{\mathrm{eff}} = 10$ for $n = 12$ to account for the six translational and rotational degrees of freedom. By use of the macroscopic identity

$$\frac{d\ln\rho(E)}{dE} = \frac{1}{T}\,, \tag{7}$$

and the approximation $C_p \approx C_v = dE/dT$ the heat capacity can be integrated to give the level density

$$\rho[T(E)] = AT(E)^{n_{\mathrm{eff}} b} e^{2n_{\mathrm{eff}} cT(E)}, \tag{8}$$

with the cluster energy

$$E = an_{\mathrm{eff}} + bn_{\mathrm{eff}}T + cn_{\mathrm{eff}}T^2. \tag{9}$$

The integration constants $a = -0.0186$ eV and A are determined by fixing the energy and level density at the Debye temperature ($\omega_D = 380$ K $= 0.0327$ eV [24]) to the value of a Debye crystal. The final expression for atomic evaporation reads

$$k = 4.71 \times 10^{20}\ \mathrm{s}^{-1} \frac{T_f(E)^2}{(\mathrm{eV})^2} \frac{T_f^{10b}\omega_D^b}{T_i^{11b}}\, e^{C_p(T_f) - C_p(T_i)}, \tag{10}$$

where the temperatures before and after evaporation, T_i and T_f, respectively, are determined by E and $(E - D_{13})$ via Eq. (9). Analogously, the photon emission rate is

$$k_{\mathrm{ph}}(E, h\nu) = \frac{8\pi\nu^2}{c^2}\, \sigma(h\nu) \left(\frac{T_f}{T_i}\right)^{11b} e^{22c(T_f - T_i)}, \tag{11}$$

where $T_i \equiv T(E)$ and $T_f \equiv T(E - h\nu)$. The nonlinear contributions to the caloric curve are included in the estimate of the level density. A quantum mechanical harmonic oscillator model overestimates the temperature significantly: With a Debye vibrational spectrum the error is 10% at an excitation energy of $E = 5$ eV and even 21% at $E = 8$ eV compared with Eq. (9). In addition, the use of the macroscopic heat capacity automatically includes the electronic degrees of freedom [25].

Since k_C^{-1} is the time for cluster cooling by $\simeq 0.7$ eV and since the average energies of radiated photons are $\overline{h\nu} \simeq 0.35$–$0.8$ eV for the present cluster excitation energies one may assume that the emission of one cooling photon quenches fragmentation almost completely. The measured data in Fig. 3 should thus correspond to the total photoemission rate, Eq. (4) (dotted line in Fig. 3). Although the trend is well reproduced, it tends to underestimate the observed rate by a factor of 4.

Therefore, a Monte Carlo simulation of the competing cooling channels (photon and atom emission) has been performed as follows: The initial, thermal energy is generated with a (Gaussian) distribution for room temperature and $h\nu_{\mathrm{pump}}$ added at $t = 0$. The energy of the emitted photon is simulated according to the distribution given by Eq. (11). The branching between photon and atom emission is calculated with Eq. (10) and the integral of Eq. (11), i.e., Eq. (4). The times for photon and atom emission are selected stochastically from an exponential distribution with the rate constant $k_{\mathrm{tot}} = k + k_{\mathrm{ph}}$ This process is repeated after each photoemission. After the pump-probe delay period Δt the energy of the second photon, $h\nu_{\mathrm{probe}}$, is added. The decay processes are followed through an additional 20 ms, i.e., the experimental ion storage duration after the probe laser pulse. If dissociation occurs at any point during this sequence the cluster is counted as a fragment. The fragment yield was simulated with 10^4–10^5 starting clusters for each pump/probe photon-energy combination and for each Δt value ranging from 1 μs to 1.4 s spaced by a factor of 1.5.

The simulation was performed in a two-parameter space: A scale factor s of the photoabsorption cross section was introduced through $\hat{\sigma}(\lambda) = \sigma(\lambda/s)$ in order to account for the uncertainty due to the Mie-spectrum assumption and possible quantum size effects. The factor s was varied between 0.5 and 2.0 in steps of 0.1. D_{13} was varied between 4.0 and 5.8 eV in steps of 0.1 eV. The resulting decay curves were compared to the experimental data on a point-to-point basis, and the reduced mean square deviation (χ^2) was calculated as a measure of the agreement. The best fit ($D_{13} = 5.4$ eV and $s = 1.1$,

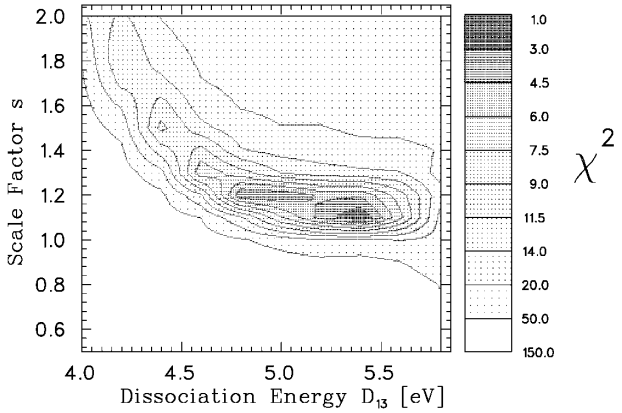

FIG. 4. Contour plot of χ^2 values as a function of the scale factor s and the dissociation energy D_{13}.

Fig. 4) shows good agreement with the experimental data (Fig. 3, solid line). The uncertainty in the emission spectra causes a systematic uncertainty in the value of the dissociation energy, possibly exceeding 10%.

The small discrepancies at low and at high energies are most likely due to a minor difference in the emission spectrum as compared to the scaled ($s = 1.1$) Mie spectrum. The dissociation energy is close to the bulk heat of vaporization of 5.3 eV [26] and the value of 4.6(3) eV of an earlier collision experiment [27], although in the latter neither radiation effects nor the temperature dependence of the heat capacity was considered. For comparison, the simulation of the cooling rates for $D = 4.6$ eV and $s = 1.0$ has been included in Fig. 3 (dashed line). In spite of the fact that the optimum scale factor of $s = 1.1$ is close to the classical value $s = 1.0$, the difference is significant in view of the steep slope of the χ^2 surface around the minimum. Such a shift has also been seen in measurements of the photoabsorption of niobium clusters [28].

To summarize, we have measured the radiative cooling of a size-selected metal cluster, V_{13}^+, with well-defined energies through the quenching action of the radiative energy loss on the evaporative loss of atoms. Radiation is found to be an effective means of energy dissipation of photoexcited clusters and thus in strong competition with atom evaporation. A Monte Carlo simulation which includes both deexcitation channels is in good agreement with the experimental values.

We thank the Deutsche Forschungsgemeinschaft for financial support.

*Present address: Forschungszentrum Karlsruhe, INE, Postfach 3640, D76021 Karlsruhe, Germany.
†Present address: Institut de Recherches Subatomiques, Université Louis Pasteur, F-67037 Strasbourg, France.

[1] R. Scholl and B. Weber, in *Physics and Chemistry of Finite Systems: From Clusters to Crystals*, NATO ASI, Ser. C, Vol. 374 (Kluwer Academic, New York, 1992), p. 1275.
[2] U. Frenzel, A. Roggenkamp, and D. Kreisle, Chem. Phys. Lett. **240**, 109 (1995).
[3] R. Mitzner and E. Campbell, J. Chem. Phys. **103**, 2445 (1995).
[4] E. Rohlfing, J. Chem. Phys. **89**, 6103 (1988).
[5] E. Kolodney, A. Budrevich, and B. Tsipinyuk, Phys. Rev. Lett. **74**, 510 (1995).
[6] K. Hansen and E. Campbell, J. Chem. Phys. **104**, 5012 (1996).
[7] J. U. Andersen, C. Brink, P. Hvelplund, M. Larsson, B. Bech-Nielson, and H. Shen, Phys. Rev. Lett. **77**, 3991 (1996).
[8] J. Laskin, C. Weikhardt, and C. Lifshitz, Chem. Phys. Lett. **277**, 564 (1997).
[9] V. Weisskopf, Phys. Rev. **52**, 295 (1937).
[10] L. Schweikhard *et al.* (to be published).
[11] S. Becker *et al.*, Rev. Sci. Instrum. **66**, 4902 (1995).
[12] G. Savard *et al.*, Phys. Lett. A **158**, 247 (1991).
[13] C. Walther *et al.*, Z. Phys. D **38**, 51 (1996).
[14] J. Faulk and R. Dunbar, J. Phys. Chem. **93**, 7785 (1989).
[15] C. Walther *et al.*, Chem. Phys. Lett. **256**, 77 (1996).
[16] G. F. Bertsch, N. Oberhofer, and S. Stringari, Z. Phys. D **20**, 123 (1991).
[17] S. Frauendorf, Z. Phys. D **35**, 191 (1995).
[18] P. A. Hervieux and D. H. E. Gross, Z. Phys. D **33**, 295 (1995).
[19] K. Hansen and E. Campbell, Phys. Rev. E **58**, 5477 (1998).
[20] C. Walther *et al.* (to be published).
[21] G. Mie, Appl. Phys. **4**, 25 (1908).
[22] C. Kittel, *Introduction to Solid State Physics* (John Wiley & Sons, New York, 1995).
[23] D. R. Lide, *Handbook of Chemistry and Physics* (CRC Press, Boston, 1995), 75th ed.
[24] R. Meyer, *Gmelins Handbuch der anorganischen Chemie* (Verlag Chemie GmbH, Weinheim, 1968), 48th ed.
[25] K. Hansen and M. Manninen, J. Chem. Phys. **101**, 10 481 (1994).
[26] A. N. Nesmeyanov, *Vapor Pressure of the Chemical Elements* (Elsevier, Amsterdam, 1963).
[27] C.-X. Su, D. Hales, and P. Armentrout, J. Chem. Phys. **99**, 6613 (1993).
[28] M. B. Knickelbein and W. J. C. Menezes, Phys. Rev. Lett. **69**, 1046 (1992).